Progress in Disaster Science 10 (2021) 100159

Contents lists available at ScienceDirect

Progress in Disaster Science

journal homepage: www.elsevier.com/locate/pdisas

Regular Article

Changing significance of landslide Hazard and risk after the 2015 M_w 7.8 Gorkha, Nepal Earthquake

Nick Rosser [a,*], Mark Kincey [a], Katie Oven [b], Alexander Densmore [a], Tom Robinson [c], Dammar Singh Pujara [d], Ram Shrestha [d], Jakub Smutny [e], Kumar Gurung [e], Sundup Lama [f,1], Megh Raj Dhital [f]

[a] Department of Geography, Durham University, Lower Mountjoy, South Road, Durham DH1 3LE, UK
[b] Department of Geography and Environmental Sciences, Northumbria University, Newcastle upon Tyne NE1 8ST, United Kingdom
[c] School of Geography, Politics and Sociology, Newcastle University, Newcastle upon Tyne NE1 7RU, UK
[d] NSET, Sainbu Bhainsepati Residential Area, Lalitpur, Lalitpur 13775, Nepal
[e] People in Need Nepal, Ranibari Marg, Kathmandu 44600, Nepal
[f] Central Department of Geology, Tribhuvan University, Kathmandu 44618, Nepal

ARTICLE INFO

Article history:
Received 14 December 2020
Received in revised form 23 February 2021
Accepted 24 February 2021
Available online 2 March 2021

Keywords:
Earthquake-triggered landslides
Post-seismic hazard and risk
Satellite mapping

ABSTRACT

The 2015 M_w 7.8 Gorkha, Nepal Earthquake triggered in excess of 20,000 landslides across 14 districts of Central and Western Nepal. Whilst the instantaneous impact of these landslides was significant, the ongoing effect of the earthquake on changing the potential for rainfall-triggered landsliding in the months and years that followed has remained poorly understood and challenging to predict. To provide insight into how landsliding has evolved since the earthquake, and how it has impacted those living in the affected area, a detailed time-series landslide mapping campaign was undertaken to monitor the evolution of coseismic landslides and the initiation of new post-seismic landslides. This was supplemented by numerical modelling to simulate the future potential reactivation and runout of landslides as debris flows under monsoon rainfall, identifying locations potentially at risk. This analysis shows that landslide hazard was higher in November 2019 as compared to immediately after the 2015 earthquake, with a considerable portion of the landscape being impacted by landsliding. We show that, while pre-existing landslides continued to pose the majority of hazard in the aftermath of the earthquake, a significant number of landslides also occurred in new locations. We discuss the value of this type of analysis in informing the reconstruction and management of settlements at risk by summarizing how this work was integrated into the project Durable Solutions II, that supported communities at risk from landslides. Finally, we consider how such data could be used in future to inform risk sensitive land-use planning and disaster recovery, and to mitigate the impacts of future landsliding in Nepal and beyond.

1. Introduction

As of September, the rate and severity of monsoon-triggered landsliding in 2020 in the earthquake-affected districts of Central and Western Nepal has exceeded that witnessed in each year since 2015. Whilst the underlying causes for this extremely severe landslide season are complex, this in part is suggested to reflect the high monsoon strength [37], the negative consequences of extensive poorly planned rural infrastructure development on landsliding [29], and the legacy impacts of ground damage generated by the 2015 earthquake [19]. To the end of September, the 2020 monsoon resulted in 83 fatal landslides resulting in the loss of more than 240 lives, according to Government of Nepal data collated via the bipad disaster information management system.[2] These figures suggest both a greater number of fatal landslides than average, and also a greater average impact per landslide during this season, as compared to both the 2015–2019 period and the longer-term historical data for Nepal [14,37].

Several tragic examples from the summer of 2020 exemplify the high level of hazards and risks posed by landsliding in the area affected by the 2015 earthquakes, even five years later. On 9 July 2020, two debris flows occurred in the Almo Thado and Kabre Kholas (*khola*: river) just north of Barhabise, Sindhupalchok, destroying the settlement of Jambu (Barhabise Municipality-5) and resulting in 23 fatalities.[3] The settlement had grown rapidly in recent years parallel to the Arniko Highway, associated primarily with the nearby power-house of the Middle Bhote Koshi Hydropower

* Corresponding author.
E-mail addresses: n.j.rosser@dur.ac.uk (N. Rosser), m.e.kincey@dur.ac.uk (M. Kincey), katie.oven@northumbria.ac.uk (K. Oven), a.l.densmore@dur.ac.uk (A. Densmore), tom.robinson1@newcastle.ac.uk (T. Robinson), dpujara@nset.org.np (D.S. Pujara), ramshrestha@nset.org.np (R. Shrestha), jakub.smutny@peopleinneed.cz (J. Smutny), kumar.gurung@peopleinneed.cz (K. Gurung).
[1] formerly of People in Need Nepal, Ranibari Marg, Kathmandu 44600, Nepal

[2] bipadportal.gov.np, the NDRRMA disaster information management system (accessed 13.11.20)
[3] https://www.nepalitimes.com/latest/nepals-deadliest-monsoon-in-recent-times/ (accessed: 7.9.20)

http://dx.doi.org/10.1016/j.pdisas.2021.100159

Project, with many houses on land directly adjacent to the khola. The event occurred as a result of a cloud-burst that triggered extensive but shallow landsliding on the hillside above the settlement that transitioned to debris flows that ran out down the channel network (Fig. 1). The landsliding may have been exacerbated by recent road construction that intersected the channel network on the hillside above the settlement.

A second significant event occurred in the village of Lidhi (Jugal Municipality) on 14 August 2020, resulting in the loss of 37 lives and destroying around 37 houses[2]. Here again, a shallow rainfall-triggered landslide failed above the village in an area that had exhibited cracking since the 2015 earthquakes. The landslide entrained soil from the terraces in its path, destroying the flank of the settlement (Fig. 1). Local concerns had been reported about the potential for landsliding in Lidhi before the event, with the community relocating overnight to reduce the risks. The settlement was also identified in the National Reconstruction Authority (NRA) Geohazard Assessment as potentially at risk from landslides, but mitigation rather than relocation was considered the most suitable risk reduction measure at the time of the assessment.

This level of landslide activity raises a series of critical observations that are fundamental to consider if the loss of life due to rainfall triggered

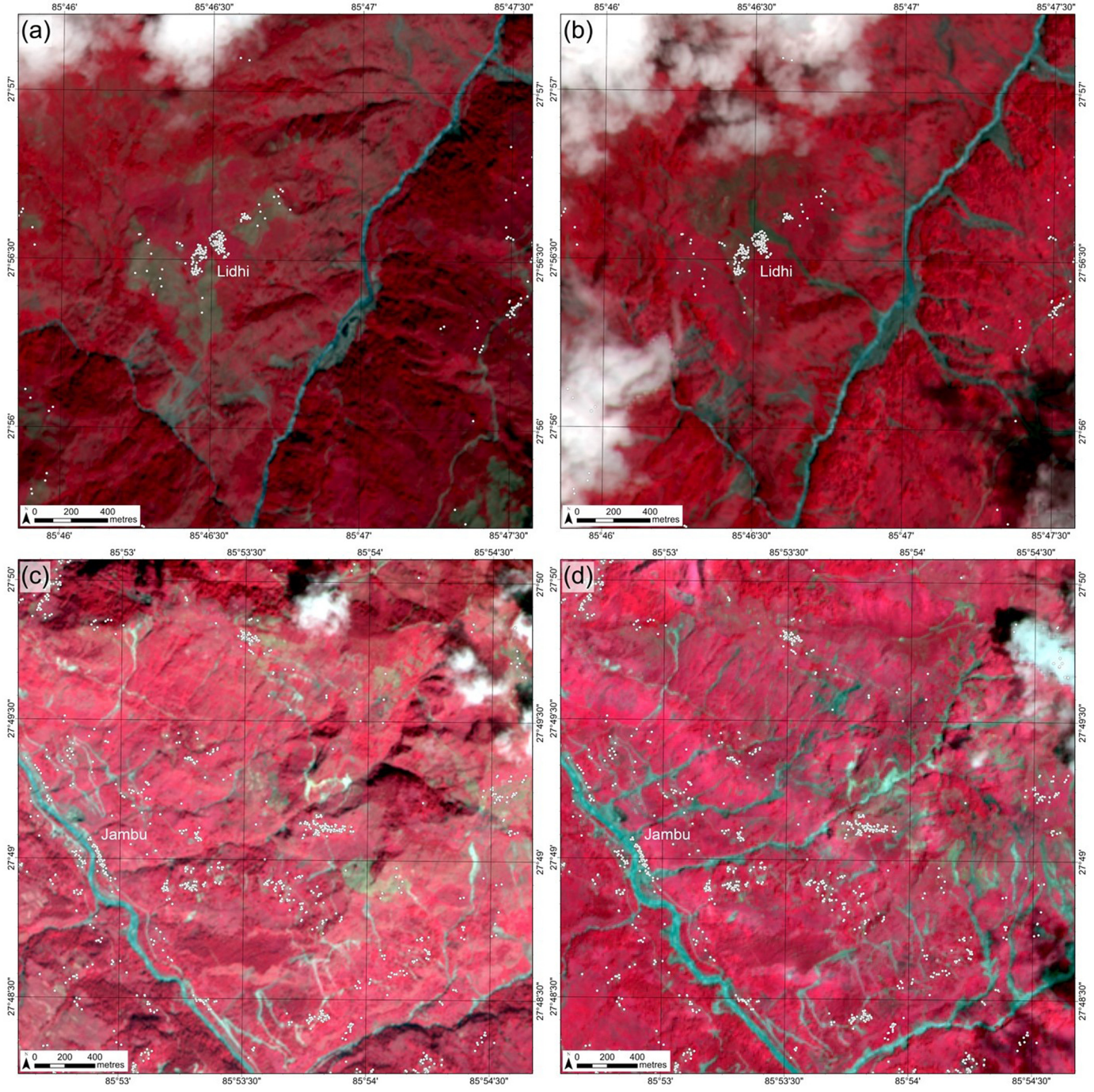

Fig. 1. (a) Sentinel-2 satellite image dated 15/10/19, displayed in false colour (bands 8–4-3) for Lidhi (Jugal, Ward 2, Sindhupalchok) (Copernicus Sentinel data [2020]. Retrieved from: [7 September 2020], processed by ESA). White dots show house locations from OpenStreetMap and Central Bureau of Statistics data. (b) Sentinel-2 satellite image for the same area dated 23/8/20, after the landslide on 14/8/20, showing the landslide that impacted the village, but also several other new landslides in the area. (c) Sentinel-2 satellite image for the area around Jambu (Barhabise Municipality-5) 15/10/19, and, (d) Sentinel-2 satellite image for the same area dated 20/8/20, showing extensive landslide impacts of a cloud burst on 9/7/20.

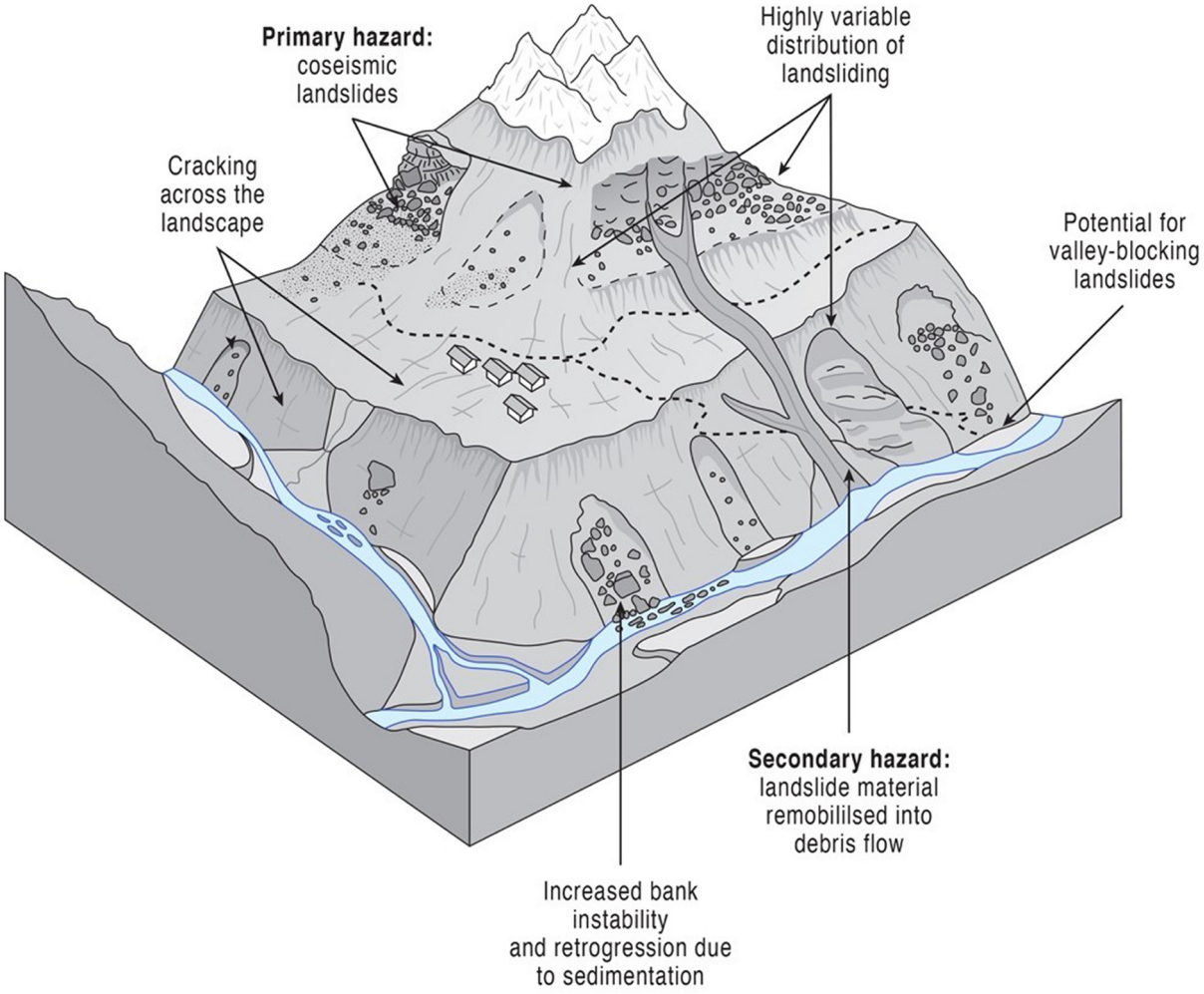

Fig. 2. Schematic block diagram illustrating typical characteristics of coseismic and post-seismic landslides (not to scale).

landsliding in Nepal is to be reduced. Whilst the impacts were devastating and resulted in an exceptionally significant and tragic loss of life, the landslides which led to these events were by no means exceptional both in terms of size and style: both disasters were driven by shallow, rapid, rainfall-triggered landslides that have been demonstrated to drive the majority of the annual losses associated with landsliding in Nepal [14]. Although not large in a geological sense, these landslides are however of a scale where physical mitigation through engineering would be highly challenging in any country, and especially so in a developing country context with limited resource and technical capacity; stopping such a landslide is therefore likely an unrealistic goal.

The timing of the highest landslide risk conditions annually is relatively well-understood [37] and each of these landslides occurred early in the monsoon, when the peak of landslide fatalities has been recorded every year [37]. Despite this, targeted early warnings for such events remain immensely challenging: regional-scale ('territorial') landslide early warning systems [21] lack the local specificity to predict exactly which slope will fail, and in Nepal are limited by the lack of hydrometeorological infrastructure to underpin such warnings. There is also a lack of reliable and affordable approaches to slope-specific landslide early warning systems [42], with arguably no examples of lives actually being saved by a landslide early warning in Nepal. Given this uncertainty, a more precautionary approach of identifying and then supporting at-risk settlements to relocate to safer places is a more reliable risk reduction measure. This requires good geospatial knowledge of landslide risk and a willingness to move. In a context where limited and constrained choices of resettlement options interleave with competing demands on livelihoods and land-ownership, simply relocating to apparently lower-risk areas is immensely complicated [33].

Finally, the events of the 2020 monsoon demonstrate the dynamic nature of landslide risk in the aftermath of a large earthquake. Whilst landslide hazard assessment is difficult in steep topography with a monsoonal climate, it is made even more challenging given limited scientific and practitioner experience of how earthquake damage affects future landslide hazard and risk [13,35]. In this paper we provide a summary of research that has been conducted across the 14 districts identified by the Government of Nepal as those most severely impacted by the 2015 earthquakes. We focus on the district of Sindhupalchok, to consider how landslide hazard and risk have evolved since 2015, and how this risk can or could be reduced. We begin by providing a short review of current scientific understanding of the nature of coseismic (earthquake-triggered) landsliding and how this evolves through the years that follow the initial earthquake shaking. We then describe a program of research that has used satellite imagery to map the evolution of landsliding up until post-monsoon 2019. We summarise the findings of this work to show how landsliding has evolved, and the consequences for this on the risks that people face. We describe how the findings were integrated within the Durable Solutions II project that supported communities at risk from geohazards after the 2015 earthquakes. We distil a series of observations on the nature of post-earthquake landslide hazard and risk and demonstrate where and when landslide risks can be reduced through improved land-use planning, and where and when this becomes more problematic.

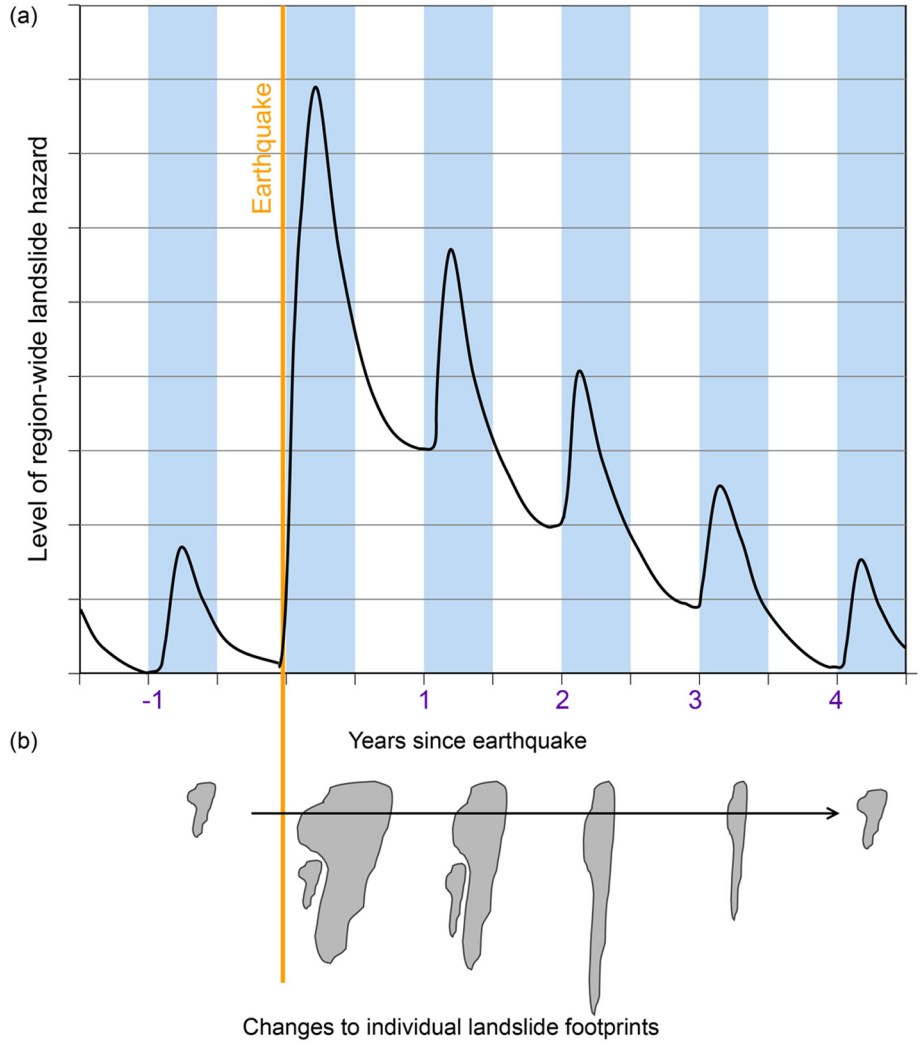

Fig. 3. Conceptual diagram of the evolution of post-seismic landslide hazard, based on understanding gained before the Gorkha earthquake. **(a)** shows years since the earthquake (orange line), and the change in regional landslide hazard through time. Plot shows typical peak in landslide hazard (black line) early in each monsoon season (shown by the blue bars), and how this is anticipated to change as a result of the Gorkha earthquake. **(b)** shows how individual landslide footprints may change through time, from small landslides before the 2015 earthquake, to larger landslides after, and in particular an elongation as landslide debris is remobilised into debris flows in subsequent monsoons. The period over which the return of landsliding to pre-earthquake levels remains poorly understood and is shown only schematically here.

1.1. The nature of coseismic landsliding

Coseismic landslides are the most significant secondary hazard associated with high-magnitude continental earthquakes [13]. Widespread landsliding has been documented after numerous large earthquakes, and such landslide-triggering events are known to result in substantially higher death tolls than earthquakes without landslides [6]. The consequences of coseismic landsliding includes wider disruption to infrastructure [3,5], and the transport of large volumes of sediment into the fluvial network [47]. Much research has focused on the characterization of coseismic landslides, which has led to an improved understanding of their spatial distribution, impact, and style. This insight has been gained from the development of mapped coseismic landslide inventories that describe landslide location and extent [45].

Despite a growing number of studies that have documented coseismic landsliding, far less is known about how landsliding evolves post-earthquake. Examples from recent significant earthquakes, notably the 1999 M_w 7.6 Chi-Chi earthquake in Taiwan and the 2008 M_w 7.9 Wenchuan earthquake in China, reveal a persistence of enhanced landslide rates, and long-term impacts of coseismic hillslope damage, in the years to decades after the shaking (e.g., [9,16,25,35]). This work has started to document two key landslide processes (Fig. 2). The first is the continued instability, activity and eventual stabilization or exhaustion of landslides that were triggered by the earthquake. The second is the occurrence of new landslides in the months or years after the earthquake, often in response to intense rainfall, but importantly also as a direct result of coseismic damage to the ground. The timescale over which such new landsliding occurs, and remains over and above 'normal' conditions, is poorly constrained, mainly because there are only a small number of well-documented examples from a limited range of tectonic and physiographic settings. For example, analysis of suspended sediments in the fluvial network and time series landslide mapping following Chi-Chi suggested a post-seismic reduction in sediment flux [16], with the rate of new landsliding [25] returning back to pre-event levels within approximately six years after the earthquake. Conversely, research on vegetation recovery following landsliding during the 2008 Wenchuan earthquake suggests a more extended and complicated response over periods of decades rather than years (e.g., [52]).

This concept of a landslide 'recovery time' is a critical factor in post-seismic landslide hazard assessment as it determines the likely time period over which enhanced landsliding should be expected. However, the interplay and dominance of each of these two forms of landsliding remain poorly documented, and consequently how post-seismic landslides evolve, and the

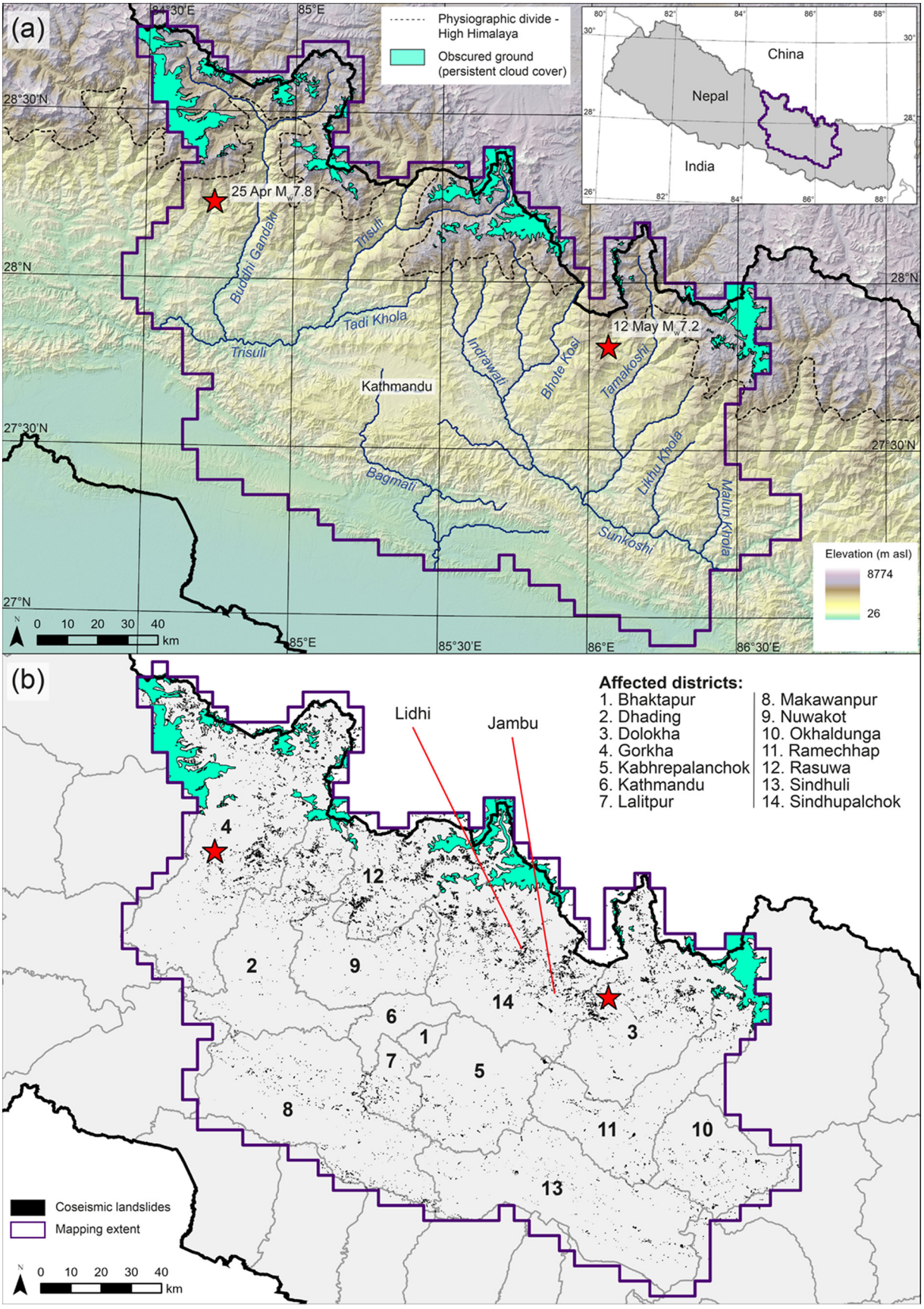

(*caption on next page*)

hazard that they pose, is poorly understood (e.g., [41,49]). Nevertheless, previous research has provided several key insights into the nature of coseismic landsliding that are pertinent to understanding the post-seismic landslide hazard and risk, described below.

1.2. The hazards posed by coseismic landslides in the aftermath of an earthquake

The nature of landslides triggered by earthquakes is known to markedly differ from landslides typically triggered by rainfall [13]. This difference is key in identifying the likely location, nature and timing of landslides in the period following an earthquake, and hence the hazard that they pose, as shown in Fig. 2. The main characteristics of relevance include:

(1) Coseismic landsliding is not uniformly distributed and is typically characterized by the preferential failure of specific parts of the landscape [31]. For example, an asymmetry in the density of landslides on slopes directed towards the seismic source versus those facing in the opposite direction has been previously demonstrated [41]. It follows that future landsliding may follow a similar spatial pattern. Similarly, ridgelines and convexities generate localized amplification of seismic waves [12], triggering many landslides high on valley sides (e.g. [39]). As a result, and particularly in earthquakes which occur during dry soil moisture conditions, much landslide debris released during earthquakes can remain perched high in the landscape, posing a significant potential future hazard.

(2) Landslides triggered by earthquakes can be very different in mechanism compared to those triggered by rainfall. As a result, these landslides may behave very differently during later rainfall. This was typified in the Gorkha earthquake, where many deep-seated rainfall-triggered landslides that pose perennial disruption in the Middle Hills showed almost no sign of accelerated movement during the earthquake itself (e.g., [4]). Conversely, coseismic landslides typically include shallow failures in regolith or weathered bedrock, rockfall, deeper-seated failures triggered by liquefaction, and spreading due to intense localized shaking ([28]). Critically, coseismic landslides and the debris that they release are very sensitive to rainfall, reducing the post-earthquake intensity-duration threshold for debris-flow triggering [67]. In this context, the degree to which (local) knowledge and lived experience of pre-earthquake landslide hazards remains germane in a post-earthquake setting is poorly understood [1,33].

(3) It is widely acknowledged that earthquake shaking can generate extensive damage to the ground through cracking (commonly termed *ground cracking* (e.g. [17]), *fissuring* (e.g. [34]) or *lateral spreading* (e.g. [8])), resulting in a net reduction in material strength even in areas that show little or no obvious surface evidence of landsliding. In the aftermath of the Gorkha earthquake, many slopes were observed to have surficial cracks, suggesting a potential incipient landslide. To date, there is very limited research on the degree to which such surface disruption can be taken as an indicator of future risk [28,36], and how such damage influences slope stability and future landslide hazard.

The consequences of these factors for post-seismic landslide hazard are twofold. Firstly, and most importantly, the hazard posed by the reactivation of coseismic landslides can be assessed with some degree of confidence; where coseismic landslides are mapped, the future risks posed by their reactivation and runout can be modelled using established flow-routing algorithms. It is therefore critical to identify, repeatedly map and assess the potential for runout at these locations. At present, however, it is not known if this type of landsliding poses a significant component of the overall hazard faced in the aftermath of an earthquake. If it does, then this type of assessment could be used to significantly reduce net landslide risk in the years that follow. Secondly, and more challenging, is the assessment of likely locations of new landslides in previously (apparently) stable locations. Key to this is understanding the overlay of earthquake damage and existing landslide susceptibility, to identify how post-seismic landsliding is distributed across the landscape, and, critically, how this evolves through time.

This complexity is simplified in a conceptual model (Fig. 3). The annual concentration of rainfall-triggered landsliding around the start of the monsoon, followed by an asymptotic decay back to background levels as the monsoon recedes, is well-understood. The manner in which this pattern – either regionally across the area impacted the earthquake (Fig. 3a), or locally for an individual hillslope or landslide (Fig. 3b) - responds after the earthquake is largely unknown. Based on previous research, it was anticipated that the reactivation of landslides triggered by the earthquake and new landslides as a result of the damage to the wider landscape would result in exacerbated landsliding in the 2015 monsoon. It was also anticipated that the remobilization of coseismic landslide debris in the monsoon would lead to increased numbers of debris flows [10]. Critically, the period over which these processes are anticipated to persist above 'average' (months, years or decades), and the changes in the year-on-year intensity of landsliding, remain unknown. Encompassing this is also a wider social and political context and the consequent human-environment links that aggravate landsliding [37,43]. For example, the post-earthquake period saw massive investment in reconstruction, but also the proliferation of rural road construction that was at least anecdotally associated with the first local elections in 2017 [50]. The key unknown here is, given this wider ongoing change, whether the pre-earthquake landslide conditions might ever be regained.

1.3. Coseismic landsliding associated with the Gorkha earthquake

The Gorkha earthquake initiated ~80 km northwest of Kathmandu, with the rupture propagating east ~140 km along the Main Himalayan Thrust (MHT) [2]. A series of aftershocks followed, including a M_w 7.3 event on 12 May ~75 km east-northeast of Kathmandu close to the border between Sindhupalchok and Dolakha districts. The intense shaking generated by the earthquake triggered extensive landsliding across the full east-west extent of the fault rupture. The density of landslides (the number or area of landslides per unit area) generally increased towards the eastern margin of the rupture [19,27]. Multiple coseismic landslide inventories have been generated since the earthquake (e.g. [18,27,51,46,40,49,30,19], resulting in a range of estimates of coseismic landslide numbers ranging from <5000 to ~25,000. The number varies based upon the mapping techniques, the satellite imagery, and the choices made in the generation of the inventories (see: [19]). The most spatially detailed assessment using high resolution optical satellite imagery, and therefore probably the most complete inventory to date, was generated by Roback et al. [40], who mapped ~25,000 landslides, covering around ~90 km^2 and distributed across 28,300 km^2 of Central and Western Nepal.

1.4. National reconstruction authority, the geohazards assessment and durable solutions II

Following the earthquakes in 2015, and after the recognition of the severity of the landslide impact triggered by the event, the Government of Nepal began an assessment of the landslide hazard and associated risk to feed into the response and reconstructions efforts, termed the Geohazards Assessment. This involved an initial series of field assessments led by the

← **Fig. 4. (a)** Study area extent in central and western Nepal (purple boundary), covering the area impacted by coseismic landslides associated with the Gorkha earthquake. Stars show the epicentres of the Gorkha earthquake sequence: 25 April M_w 7.8 and 12 May M_w 7.2. Shaded relief elevation map derived from a 30-m ALOS DEM of the study area (Credit: AW3D30 – JAXA). **(b)** Mapped coseismic landslide inventory, with landslides shown as black polygons. The locations of the Lidhi and Jambu case studies in Sindhupalchok (Fig. 1) are labelled. Modified from Kincey et al. [19].

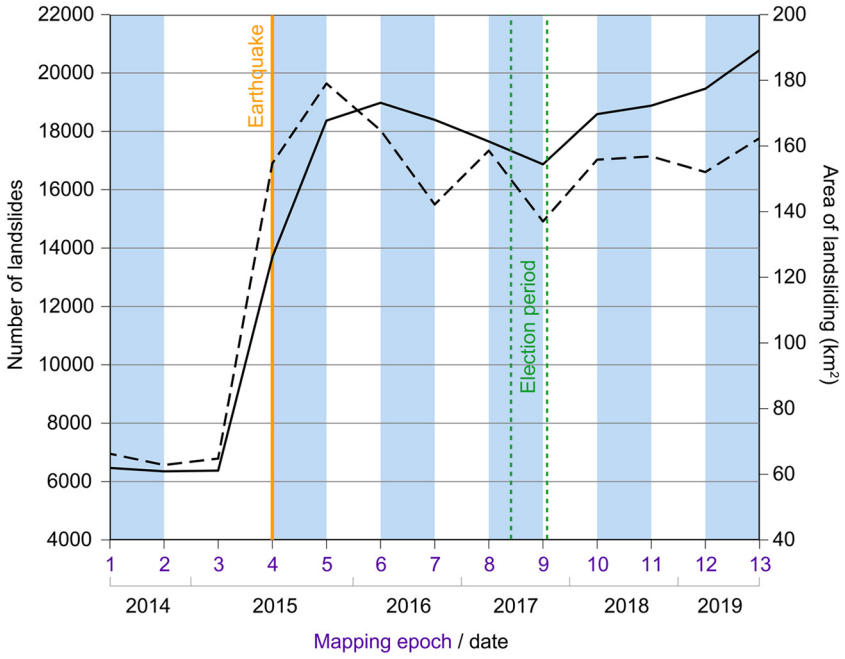

Fig. 5. Changes in mapped landslide numbers and total landslide area between 2014, the Gorkha earthquake in 2015, and post-monsoon 2019. Vertical blue bars show the timing of the monsoon; solid black line is landslide number; dashed black line is landslide area; and, the time of the earthquake (orange line) and the first local elections are indicated by orange and green lines respectively. Modified from Kincey et al. [19].

Department of Mines and Geology, reaching around 130 settlements. The identification of these settlements for the assessment was based on requests made by local government officers, where a potential risk had been recognized. A further round of assessments followed, reaching a further 455 locations across 15 districts, as part of the National Reconstruction Authority (NRA), with support from the UN Office for Project Services (UNOPS) in Kathmandu, which involved around 40 geologists and engineers undertaking detailed site visits. These assessments resulted in a three-tier categorization: Category 1, 'Safer communities / villages where reconstruction can be started any time'; Category 2, 'Communities / villages under the risk of manageable geohazards where reconstruction could be started only after applying suitable countermeasures'; and Category 3, 'Unsafe communities/villages due to the existing state of geohazards which are extremely difficult to control technically as well as financially where reconstruction is not recommended.' The assessment documented the number of households requiring relocation where deemed necessary to reduce the risk to an acceptable level, as well as outlining recommendations for remedial mitigation, and identifying the responsible government agency to take this forward in Category 2 locations. The geohazards assessment was extended in the Durable Solutions program,[4] led by People In Need, acting as a bridge between government and communities affected by landslides to support fair and voluntary relocation.

Since this initial effort, a larger number of additional sites have been evaluated, and some reassessed, notably where concerns were raised about recent deterioration in a landslides condition. As of July 2020, a total of 1053 sites had been assessed. Of these sites, 40% (419 sites) were Category 1, 30% (320 sites) Category 2, and 30% (314 sites) Category 3, with more than 4000 households recommended for relocation.

While this rapid appraisal was an essential component of the assessment of geohazard risk, it was inevitably a single snapshot in time that did not capture the dynamic changes in landslide hazard. This effort also depended on local recognition and then reporting of sites at risk. This was made all the more challenging by the remote rural expanse of the affected districts, and the competing demands of the post-disaster context. Given the lack of precedent for assessing the future threat posed by landslide hazards, plus the uncertainties around how ground damage accrued in the earthquake might develop into landsliding, it was challenging for local government, householders, and technical specialists to assess the likely future risks.

2. Mapping the evolution of coseismic landsliding after the Gorkha earthquake

In order to complement the Geohazards Assessments, and to provide a spatially continuous and updating assessment of landsliding after the Gorkha earthquake, systematic mapping using freely available satellite imagery was developed. The intention was to develop a sustainable and consistent method to generate reliable and repeatable landslide information, with the specific intention of assessing change through time at a scale relevant to individual households. Whilst some mapping efforts (e.g., [40]) have exploited very high-resolution optical imagery allowing very small features (< 5 m) to be identified, the low orbit height of these satellites results in considerable topographic image distortion (up to >100 s of m), particularly in high-relief topography. This makes change detection difficult, because the errors in image rectification far exceed the changes on the ground [48]. We therefore used medium resolution (ca. 10–30 m) optical imagery with minimal distortion to provide a more reliable means of monitoring landslide change.

We manually mapped landslides from freely-available optical satellite imagery (Landsat and Sentinel-2) between 2014 and 2019, with two image periods before and after the monsoon each year and one immediately post-earthquake, yielding 13 mapping epochs. We focused on the 14 districts most affected by the earthquake, which includes around 90% of the landslide-affected area initially mapped by Roback et al. [40] (Fig. 4). Landsat 8 imagery (30 m spatial resolution, pan-sharpened to 15 m) was used for epochs 1–5 (2014–2015), and Sentinel-2 imagery (10 m spatial resolution) from epoch 6 onwards (2016–2018). Landslides were mapped on true colour (R-G-B) and false colour (NIR-R-G) composites using bands 2–3–4-5 for Landsat 8 and 2–3–4-8 for Sentinel-2.

Unlike previous multi-temporal inventories (e.g., Fan et al., 2018; [22,23,26]), we independently mapped the full extent of all landslides visible on imagery from each epoch, reducing any reliance on assumed

[4] www.durablesolutions.org (accessed: 1.10.20)

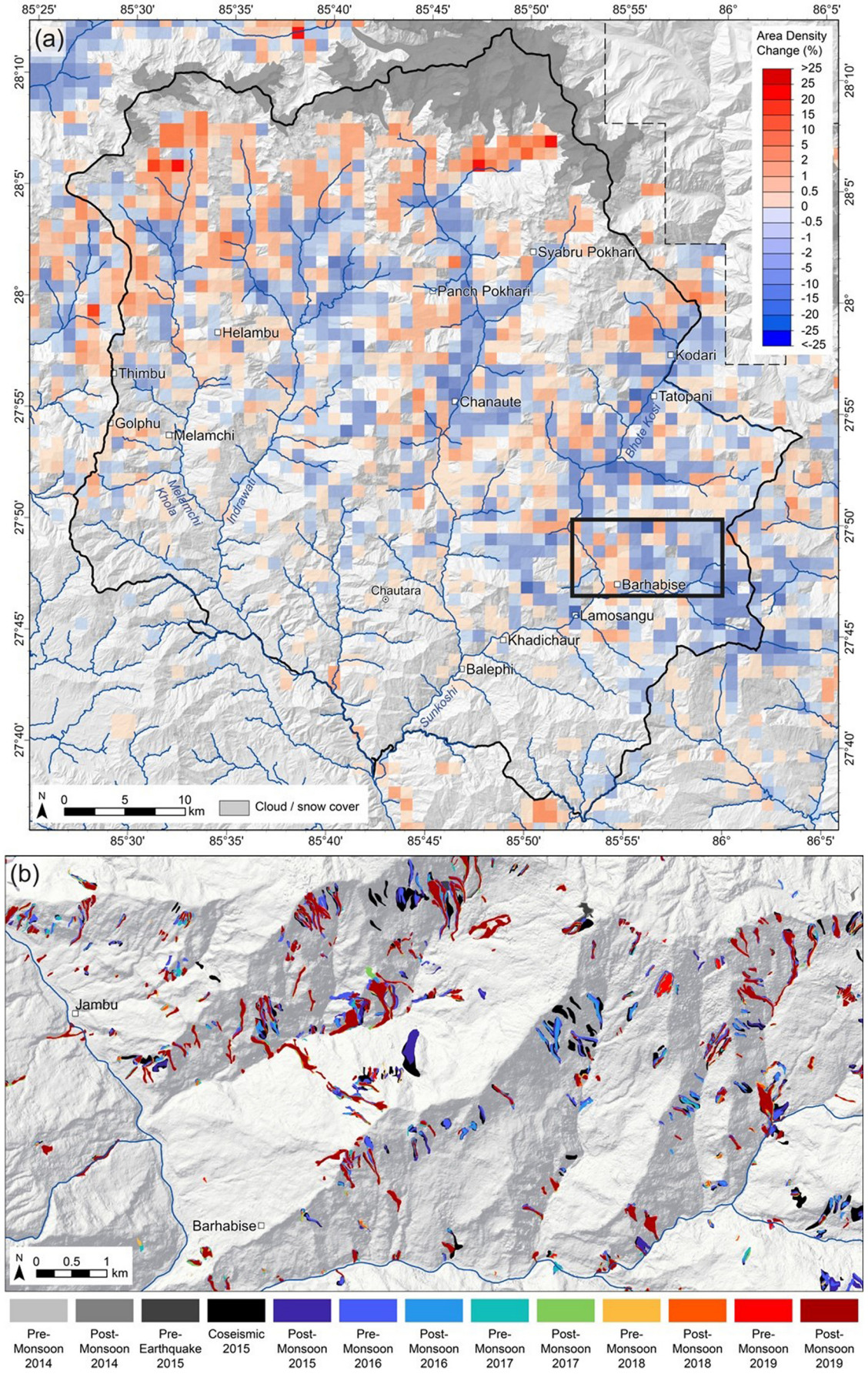

(caption on next page)

similarity or difference with the previous epochs. A common issue with large-scale multi-temporal landslide inventory analysis over mountain topography is the presence of intermittent cloud, shadow, and snow, which typically limits the area that can be assessed. Automated masking of clouds was undertaken using *Fmask* (Function of mask, v4.0) [38], which was manually checked for accuracy. Areas of persistent cloud or snow totalled 5% of the study area concentrated in the High Himalaya, coincident with areas of minimal population. For ease of comparison, landslides were summarized to areal densities (landslide area per km^2) on a 1 km^2 grid. The full methodology is provided in detail in [19].

3. Results

3.1. Summary of the landslide inventories

The landslide inventory we consider here includes 200,866 mapped landslides across all 13 epochs. Landslide numbers average ~ 6400 for all 3 pre-earthquake epochs, although the location of individual landslides change, but with little notable systematic variability between the characteristics of pre- and post-monsoon inventories (Fig. 5). The Gorkha earthquake (epoch 4) and the monsoon that followed (epoch 5) led to very significant increases in the number of mapped landslides, peaking at 18,978 in pre-monsoon 2016 (epoch 6), declining through post-monsoon 2017 (epoch 9), and increasing in both pre- and post-monsoon 2018 and 2019 (epochs 10–13). Critically, by the end of the study period, there were over 7000 more visible landslides compared to immediately post-earthquake (ca. 13,700), and over 14,000 more than the pre-earthquake inventories (Fig. 5). In this sense, landslide hazard remains significantly higher today than on the day of the earthquake, and so may reflect only the beginnings of a longer-term response to the earthquake [13,19].

Considering the areal density of landsliding, for the majority of epochs, the proportion of grid cells newly affected by landslides relative to the preceding epoch was low (1–2%), with the exception of the earthquake (10%), the 2015 monsoon (5.5%) and pre-monsoon 2018 (3%). The critical conclusion from this is that, at least at this scale of assessment (1 km^2 grid), by far the majority of changes to landsliding in the aftermath of the earthquake are concentrated near coseismic landslides, rather than in areas that did not experience landslides during the earthquake (Fig. 6a). It follows that knowledge of coseismic landslides, and if and how they evolve, is critical for understanding the majority of landslide risk in the aftermath of the Gorkha earthquake.

Superimposed on top of this preferential concentration of activity near coseismic landslides, about 11% of grid cells in the post-monsoon 2018 epoch were newly affected by landslides since the earthquake (epoch 4), indicating that the spatial pattern of landsliding had altered steadily but progressively since the earthquake. It is therefore important to recognize that the potential for additional new landsliding in previously apparently stable areas is persistent for years after the earthquake, and so better understanding of post-earthquake landslide susceptibility and how cracked and damaged ground develops into landsliding is essential.

3.2. Assessment of landslide risk to households

The sequential mapping of landslides over the period since the Gorkha earthquake shows that a considerable proportion of the overall landslide hazard can be attributed to the reactivation and remobilization of coseismic landslides. Reactivation mostly occurs during intense prolonged rainfall in the monsoon, notably as debris flows [13]. Identifying the likely pathways along which (re)mobilised sediment could travel as debris flows is therefore a crucial aspect of a timely assessment of post-seismic landslide hazard. Given the large number of landslides in the 14 earthquake-affected districts, an approach was needed that combined a synoptic regional assessment but also locally relevant detail to those potentially at risk.

The typical approach to assess regional-scale debris flow hazard is to model runout pathways based on a landslide source dataset. An assumption can be that each landslide scar has the potential to remobilize as a debris flow, and so can be considered a source. To undertake this, we compared the coseismic landslide inventory, with that mapped in November 2019 [19], to analyse the evolution of post-earthquake landslides over this 4.5-year period. We considered a 'plausible but worst case' scenario, in which intense localized rainfall triggers highly mobile debris flows, akin to the type of events that resulted in the landslides at Jambu in 2020. To do this, we used Flow-R, a distributed empirical model for regional susceptibility to debris flows [15], to assess the spatial distribution of runout probabilities across the area impacted by the earthquake. As the path of debris flow runout is highly sensitive to topography, we used a high-resolution digital elevation model (5 m AW3D), down-sampled to 10 m, as the optimum balance of resolution and noise [15]. This DEM provides improved delineation of the ephemeral hillside channel network, and local topography that may direct or divert flows to or from settlements. The parameterization of Flow-R is described in full in Kincey et al. [20], and was tuned to enhance runout to be extensive but plausible, providing a conservative modelling strategy.

The output of the modelling was a spatially continuous 10 m raster of relative debris flow probability ranging from 0 to 1 (Fig. 7). This probability surface was then overlain with household locations, collated from the Central Bureau of Statistics and revised with post-earthquake (re)locations mapped in OpenStreetMap. This intersection attributed a risk score to every household and was used to identify hotspots of at-risk buildings and locations where (1) there was a risk not described in the Geohazards Assessment, (2) where the level of relative risk diverged from the Geohazards Assessment, and (3) where risk was increasing through time (Fig. 7). This approach has been validated by cross-checking the locations of those buildings that were affected by landslide runout in subsequent epochs with the modelled relative risk score, as reported in Kincey et al. [20].

In Sindhupalchok, we mapped 2898 landslides that were triggered by the Gorkha earthquake, representing 21% of the entire inventory. The post-monsoon 2019 inventory contained 4026 landslides, an increase of 39% relative to 2015. Although the area covered by landsliding in Sindhupalchok decreased from 36 km^2 in 2015 to 30 km^2 in 2019, this still represented 1.2% of the district. The increase in landslide number between 2015 and 2019 resulted in an increased impact of landsliding over this period. Of all buildings in Sindhupalchok (n = 100,908), 299 were directly hit by landslides in the earthquake. By post-monsoon 2019, 538 had been impacted, of which 108 were impacted in both the earthquake and during post-monsoon 2019. In contrast, the modelled landslide runout risk to buildings decreased between 2015 and 2019, with a total of 3128 buildings potentially at risk following the earthquake, but only 2917 by post-monsoon 2019. Immediately following the earthquake, 84% of these at-risk buildings were in the relatively low risk category (with probability of debris-flow impact, p(I), between 0 and 0.1), with 15% at moderate risk (p(I) of 0.1–0.5) and 1% at high risk (p(I) > 0.5). The absolute numbers of buildings at risk decreased in all categories by 2019, but with a slightly higher proportion at relatively low risk (87%) compared with moderate risk (13%) and high risk (<1%) categories. A critical observation is that over this period we observe a significant interchange in individual buildings at risk in 2015 as compared to 2019; around 50% of those at risk after the earthquake were no longer at risk by 2019, but importantly as the landsliding has developed, around 50% of buildings at risk by 2019 were safe in 2015. The total number of buildings that have experienced landslide risk since the earthquake (5355) therefore continues to increase.

← **Fig. 6. (a)** Map of change in landslide area density at 1 km^2 resolution between the time of the Gorkha earthquake and post-monsoon 2018, with hot colors indicating an increase in landsliding and cold colors a decrease. Box shows area near Jambu and Barhabise in panel (b). (b) Mapped landslides colored by date for each epoch between 2014 and post-monsoon 2019, for the area around Jambu and Barhabise, Sindhpalchok (see Fig. 4b for wider context). Shaded relief elevation map derived from a 5-m ALOS DEM of the study area (Credit: © NTT DATA, RESTEC/©JAXA).

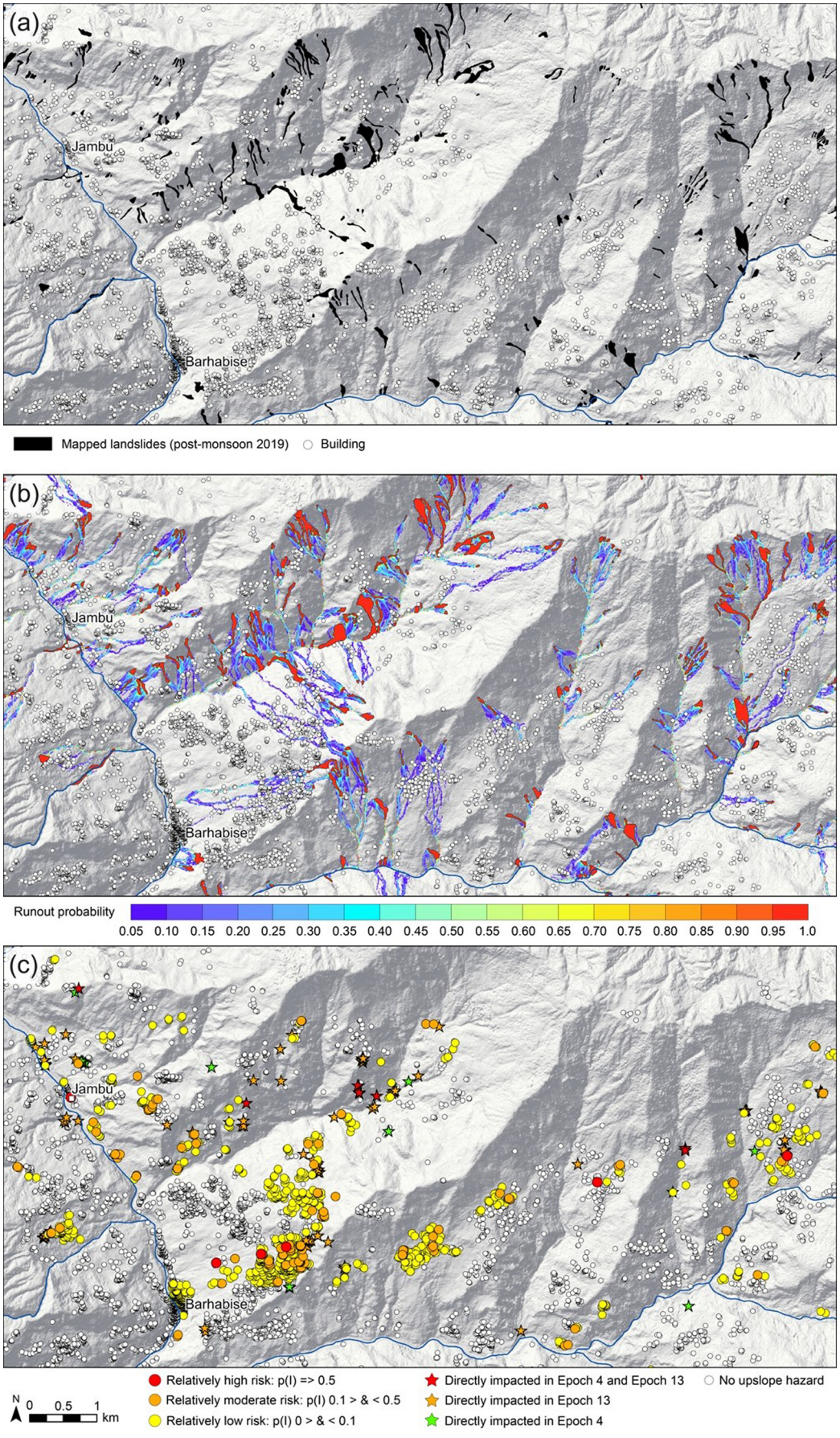

(caption on next page)

4. Discussion

We have presented a summary of the evolution of post-earthquake landslides in the aftermath of the Gorkha earthquakes. This research has shown that the landscape has not recovered as rapidly as implied by studies that focus only on the occurrence of new (additional) landslides in the earthquake aftermath (e.g., [26]), identifying a significant prevalence of hazard and risk from the reactivation of coseismic landslides. Our analysis illustrates that the nature of landslide hazard, and therefore the risk, has significantly changed since 2015. The sequential mapping demonstrates that the location of landslide activity has shifted systematically through time since the earthquake (see also [19]). The implication is that whilst the need to rebuild and reconstruct is pressing, doing so too quickly and in the absence of good data on evolving geohazards can have long-term and potentially devastating impacts on the population, property and livelihoods [33].

In detail, our results show a series of key characteristics vital in any appraisal of landslide hazard in the aftermath of a mountain region earthquake. Coseismic landslide occurrence is a reasonable first-order indicator of where future recurrent post-seismic landsliding will occur. It is critical to recognize that a substantial proportion of overall landslide threat arises from existing landslides in the landscape, and so knowing where these are and how they evolve is vital: it is not appropriate to dismiss existing landslides as 'finished' and of negligible risk. Prior to the earthquake, around 15% of the mapped 1 km^2 grid cells experienced landsliding, but this number increased to 24% following the earthquake, and then increased again to 29% following the 2015 monsoon [19]. In all years since, this proportion of cells has remained high (28–30%), so the proportion of the landscape at some degree of risk remains high.

Beyond the reactivation of coseismic landslides, nearly 10% of the landscape that did not experience landsliding on the day of the earthquake did so in the period that followed, and this as a proportion of the total increases through time. This demonstrates that the coseismic landsliding pattern should not simply be projected forward to anticipate the evolution of the hazard. It is therefore essential that indicators of future instability and changes to the landscape are monitored. Whilst the ultimate trigger of landsliding in the years that followed the earthquake was most commonly rainfall, our data strongly suggest that the pattern is linked to earthquake damage, such that these events would not have occurred if the earthquake had not happened. This attribution of fundamental cause is critical where access to compensation is reliant on precise definitions that relate specifically to the earthquake itself.

The dominance of debris flows reactivating existent landslides has a significant influence on the nature of hazard, and how this can be managed. For example, debris flows preferentially channelize, most commonly flowing from open slopes into pre-existing concavities and channel networks. Once confined within a channel, the most likely flow path is defined by pre-existing topography. Pre-existing channels therefore represent perhaps the highest risk locations in the post-earthquake landscape. This observation also reflects previously-proposed landslide hazard zonation methods, distilled into 'simple rules' from empirical analysis of the spatial characteristics of landsliding after several large earthquakes (e.g. [32]). Avoiding development in these channels is a key risk reduction measure. Related to this, risk from post-earthquake landsliding can reduce from high to negligible over very small distances (< 10 m), so precise building location matters. Similarly, it has been apparent in forensic investigations of landslide impacts after the Gorkha earthquake that new, often earthquake-resistant houses were commonly poorly located only by a matter of meters, placing them at high landslide risk. The precise positioning of a house within a plot can therefore hold a considerable influence on exposure to landslide hazards.

Landslide activity has shown little indication of a return to pre-earthquake levels, even after 4.5 years. It is clear that the legacy of the earthquake shaking holds continued influence over enhanced landslide susceptibility. Our data suggest however that a return to pre-earthquake average landslide conditions may not be simple. During this period, and particularly since 2017, we have documented an uptick in landsliding across the area, which visually from satellite imagery and anecdotally from observations on the ground appears associated with the proliferation of rural road construction around the time of the first local elections (Fig. 5). Whilst the direct impacts of rural road construction remain difficult to isolate, extrapolating what appeared to be the beginnings of a recovery in landsliding up until post-monsoon 2017 would imply that the number of landslides in the landscape should be now less than on the day of the earthquake (Fig. 5). However, in the most recent mapping we recorded c. 21,000 landslides, nearly double the coseismic number, implying that the changes to the landscape since the earthquake have had a landslide impact comparable to that of the earthquake itself. This impact is no doubt exaggerated by coseismic damage, whereby standard alignment choices and construction techniques may now be unworkable and unsustainable.

Based upon this effort, we identify several ways in which our assessment could be used in the management of future landsliding. The first is in providing regional-scale but high-resolution data on the evolution of landslides, which is essential for informing ongoing recovery and reconstruction. Further analysis could utilize physically-based modelling of the release, entrainment and transport of landslide debris through the fluvial network (e.g. [7]), feeding into consideration of the full earthquake-triggered hazard chain (e.g., [13]). Second, our landslide mapping can be used to refine regional-scale post-earthquake landslide susceptibility models that consider the whole impact footprint of the event with the detail of individual landslides, in order to improve their ability to anticipate the occurrence of new landslides over and above the capabilities of static models that do not account for seismicity. This type of susceptibility analysis is essential in contexts that lack systematically collated landslide inventories, for prioritizing areas that may face higher potential future risk. The research described here in part demonstrates the value of systematic inventories, and provides a sustainable workflow to underpin this in future. Third, our data provide an assessment of the trajectory of landslide risk for individual landslides which adds considerably to one-off site assessments.

Finally, returning to the tragic events in Jambu and Lidhi in Sindhupalchok during the 2020 monsoon season, we consider the degree to which either of these events might have been avoided or mitigated from the type of mapping and modelling outlined above. The settlement of Jambu was identified as an at-risk location in our modelling of landslide runout (Fig. 7). Landslides had been mapped in the headwaters of the Almo Thado and Kabre Kholas, and the modelling suggested that if these landslides remobilized, then the kholas would likely route the debris flows across the Arniko Highway, as happened in early July. This situation was exacerbated by a series of rural roads traversing the slope above, crossing the kholas, and apparently destablilising the surrounding hillside since the earthquake. Even without this analysis, the location of Jambu on a debris flow fan at the base of pre-existing channels shows its long-term susceptibility to debris flows. Therefore, risk sensitive land-use planning using geospatial information on hazards could be used to identify areas of potential new future landslides and where they may runout. In Jambu, for example, such approaches would identify construction on debris flow fans at the

← **Fig. 7. (a)** Footprints of mapped landslides in post-monsoon 2019, for the same area as shown in Fig. 6b. White circles show the location of buildings. **(b)** Modelled landslide runout, showing the predicted debris flow propagation under extreme rainfall, using the 2019 mapped landslides as source areas. The colour scale indicates the relative probability of any location being hit by a debris flow (white – negligible risk; blue – low risk, red – high risk). **(c)** Individual building relative risk scores extracted from the runout model, with stars indicating a direct impact. Note that the model is able to discriminate between individual houses within a single settlement. Shaded relief elevation map derived from a 5-m ALOS DEM of the study area (Credit: © NTT DATA, RESTEC/©JAXA).

mouth of steep channels as unacceptable, and therefore have the potential to help reduce exposure to such hazards in this location. Problematically, however, Jambu was one of around 10 comparable at-risk locations along just the adjacent 2 km of the Arniko Highway. Where locations for development are limited, the almost inevitable consequence is building on high risk land.

In the case of Lidhi, whilst the settlement had been identified as a Category 2 location in the NRA Geohazards Assessment with mitigation deemed sufficient to reduce the risk to an acceptable level at the time of the survey, this location was not identified in our mapping analysis. No landslide was visible above the settlement in the satellite imagery, either immediately after the earthquake or in any of the epochs mapped since. This demonstrates firstly the scientific challenge of identifying those areas damaged and at elevated levels of landslide risk across such an extensive area, particularly when the surface expression of such damage (e.g. cracks) is so limited. Secondly, this example highlights the significant value of local knowledge and observations in assessing the potential for landslide risk; observations of cracking are reported to have raised sufficient concerns for the community to relocate each night to reduce their exposure to a potential landslide if it were to occur. Attempts to relocate residents away from Category 3 communities after the Gorkha earthquake (e.g. www.durablesolutions.org) have shown the strength of attachment to place in making such decisions is immensely challenging for communities with long-term ties to land, places of cultural, livelihood and religious significance [33]. It would therefore appear that where a community has a firm conviction to relocate due to a perceived risk, that a technical assessment to affirm their perception or to reassure them of a lower level of risk should be undertaken.

5. Conclusions

Through sequential mapping of the landslides in the area impacted by the Gorkha earthquake, we have described patterns that characterize the spatial and temporal evolution of landslide hazard and risk in the period since the shaking stopped. From this we have distilled a series of observations, and here have considered these in the context of risk faced during the period of the reconstruction. Our key observations are:

- Systematic mapping of landslides in the area impacted by the Gorkha earthquake has demonstrated the value of detailed inventory data to feed into a dynamic assessment of landslide risk. This illustrates the critical value of investing in baseline data on environmental hazards, to understand pre-disaster conditions, but also to provide insight into the likely future trajectory of hazard and risk.
- Our mapping shows that the landslide hazard in the 14 worst-affected districts remains significantly higher than on the day of the earthquake in 2015. Whilst some areas have experienced a degree of stabilization, new areas have experienced landsliding and some continue to develop. Mapping and monitoring these areas is critical for informing risk sensitive land-use planning in coming years. Critically, based upon our data, it should be expected that the levels of landslide risk in these areas will remain elevated for at least several more years.
- The modelling of landslide risk due to debris flows indicates that the household-level landslide risk evolves considerably after the earthquake, with a increasing number of houses having been exposed to landslide hazard at some point since the earthquake. We identify that the most characteristic form of landsliding is a transition to debris flows, which deliver highly mobile material through hillside channels to the fluvial network. These channels represent one of the highest risk areas in the landscape. Locating houses close to these areas is therefore extremely risky, but their identification can be made from either landslide hazard and risk maps as described here, or through adopting basic principles for risk sensitive land-use planning. Critically, these risks are therefore largely avoidable.
- Two landslide disasters from Sindhupalchok in the summer of 2020 show the value of multiple approaches to assessing landslide risk in a dynamic and largely unprecedented context. What we present here is a large-scale assessment of changing risk that is intended to capture individual household conditions, by adopting a high-resolution mapping and modelling approach, but also to provide a synoptic precis of the evolving risk landscape at federal level. This however must be undertaken in tandem with on the ground, detailed geotechnical site investigations at locations of particular apparent and emerging concern. It is also essential to provide space to feed in and build upon local observations and understandings of landslide hazard and risk across the area impacted by the earthquake.

Author statement

NJR: Conceptualisation, Writing, Reviewing, Editing, Funding Acquisition; **MEK**: Methodology, Writing, Reviewing, Editing; **TR, KJO, ALD**: Writing, Reviewing, Editing; **DSP, RS**: Data Curation, Writing, Reviewing, Editing; **JS, KG, SL, MRD**: Writing - Review & Editing.

Declaration of Competing Interest

None

Acknowledgements

This research has been supported by the UKRI-DFID SHEAR program (201844-112) and NERC Urgency grant NE/N007689/1. We recognise the contributions of a wider group of analysts from Durham University who fed into various stages of the mapping campaign since 2015, post-mapping support from D Hodgson, N Cox, G Basyal, R Shrestha and M Brain, and discussions around the development of the mapping data with Prof T Bhattarai and Dr C Shrestha. We thank Dr P Horton for his support in the regional implementation of Flow-R for debris flow simulation at scale. We also thank colleagues at NSET (S Shrestha, G Jimee) and DFID (T Sumner and S Dugar). Datasets for this research are being archived with NERC's Centre for Environmental Data Analysis (CEDA), in line with the requirements of the funder, in addition to the bipad.gov.np disaster information management system. The DEM data used in the numerical modelling - AW3D - is licensed via Durham University (UK), © NTT DATA, RESTEC/©JAXA. Maps and guidance notes for use in local-level planning in Nepal that arise from this research are available at: http://community.dur.ac.uk/nepal.2015eq.

References

[1] Alexander D. Confronting catastrophe: New perspectives on natural disasters. USA: Oxford University Press; 2000.
[2] Avouac JP, Meng L, Wei S, Wang T, Ampuero JP. Lower edge of locked Main Himalayan Thrust unzipped by the 2015 Gorkha earthquake. Nat Geosci. 2015;8(9):708–11.
[3] Aydin YN, Duzgun S, Heinimann HR, Wenzel F, Gnyawali KR. Framework for improving the resilience and recovery of transportation networks under geohazard risks. Int J Dis Risk Reduct. 2018;31:832–43.
[4] Bekaert D, Handwerger AL, Agram P, Kirschbaum DB. InSAR-based detection method for mapping and monitoring slow-moving landslides in remote regions with steep and mountainous terrain: an application to Nepal. Remote Sens Environ. 2020;249:111983.
[5] Bird JF, Bommer JJ. Earthquake losses due to ground failure. Eng Geol. 2004;75:147–79.
[6] Budimir MEA, Atkinson PM, Lewis HG. Earthquake-and-landslide events are associated with more fatalities than earthquakes alone. Nat Hazards. 2014;72(2):895–914.
[7] Croissant T, Steer P, Lague D, Davy P, Jeandet L, Hilton RG. Seismic cycles, earthquakes, landslides and sediment fluxes: linking tectonics to surface processes using a reduced-complexity model. Geomorphology. 2019;339:87–103.
[8] Cubrinovski M, Bray J, de la Torre C, Olsen M, Bradley B, Chiaro G, et al. Liquefaction effects and associated damages observed at the Wellington CentrePort from the 2016 Kaikoura earthquake. Bull N Z Soc Earthq Eng. 2017;50(2):152–73.
[9] Dadson SJ, Hovius N, Chen H, Dade WB, Lin JC, Hsu ML, et al. Earthquake-triggered increase in sediment delivery from an active mountain belt. Geology. 2004;32(8):733–6.
[10] Dahlquist MP, West AJ. Initiation and runout of post-seismic debris flows: insights from the 2015 Gorkha Earthquake. Geophys Res Lett. 2019;46(16):9658–68.
[12] Densmore AL, Hovius N. Topographic fingerprints of bedrock landslides. Geology. 2000;38(4):371–4.

[13] Fan X, Scaringi G, Korup O, West AJ, van Westen CJ, Tanyas H, et al. Earthquake-induced chains of geologic hazards: patterns, mechanisms, and impacts. Rev Geophys. 2019;57(2):421–503.
[14] Froude MJ, Petley DN. Global fatal landslide occurrence from 2004 to 2016. Nat Hazards Earth Syst Sci. 2018;18:2161–81.
[15] Horton P, Jaboyedoff M, Rudaz BEA, Zimmermann M. Flow-R, a model for susceptibility mapping of debris flows and other gravitational hazards at a regional scale. Nat Hazards Earth Syst Sci. 2013;13(4):869–85.
[16] Hovius N, Meunier P, Lin CW, Chen H, Chen YG, Dadson S, et al. Prolonged seismically induced erosion and the mass balance of a large earthquake. Earth Planet Sci Lett. 2011; 304(3–4):347–55.
[17] Jibson RW, Allstadt KE, Rengers FK, Godt JW. Overview of the geologic effects of the November 14, 2016, Mw 7.8 Kaikoura New Zealand earthquake (No. 2017-5146). US Geological Survey; 2018.
[18] Kargel JS, Leonard GJ, Shugar DH, Haritashya UK, Bevington A, Fielding EJ, et al. Geomorphic and geologic controls of geohazards induced by Nepal's 2015 Gorkha earthquake. Science. 2016;351(6269) aac8353.
[19] Kincey ME, Rosser NJ, Robinson TR, Densmore AL, Shrestha R, Pujara D, et al. Evolution of coseismic and post-seismic landsliding after the 2015 Mw 7.8 Gorkha earthquake, Nepal. J Geophys Res Earth Surf. 2021;126. https://doi.org/10.1029/2020JF005803.
[20] Kincey ME, Rosser NJ, Robinson TR, Densmore AL, Horton P, Shrestha R, et al. Evolution of coseismic and post-seismic landsliding after the 2015 Mw 7.8 Gorkha earthquake, Nepal. J Geophys Res Earth Surf. 2021;126. https://doi.org/10.1029/2020JF005803.
[21] Klimeš J, Rosario AM, Vargas R, Raska P, Vicuna L, Jurt C. Community participation in landslide risk reduction: a case history from Central Andes, Peru. Landslides. 2019;16: 1763–77.
[22] Li C, Wang M, Liu K. A decadal evolution of landslides and debris flows after the Wenchuan earthquake. Geomorphology. 2018;323:1–12.
[23] Li C, Wang M, Liu K, Xie J. Topographic changes and their driving factors after 2008 Wenchuan earthquake. Geomorphology. 2018;311:27–36.
[25] Marc O, Hovius N, Meunier P, Uchida T, Hayashi S. Transient changes of landslide rates after earthquakes. Geology. 2015;43(10):883–6.
[26] Marc O, Behling R, Andermann C, Turowski JM, Illien L, Roessner S, et al. Long-term erosion of the Nepal Himalayas by bedrock landsliding: the role of monsoons, earthquakes and giant landslides. Earth Surf Dyn. 2019;7(1):107–28.
[27] Martha TR, Roy P, Mazumdar R, Govindharaj KB, Kumar KV. Spatial characteristics of landslides triggered by the 2015 Mw 7.8 (Gorkha) and Mw 7.3 (Dolakha) earthquakes in Nepal. Landslides. 2017;14(2):697–704.
[28] Massey CI, Townsend DT, Lukovic B, Morgenstern R, Jones K, Rosser B, et al. Landslides triggered by the MW7.8 14 November 2016 Kaikōura earthquake: an update. Landslides. 2020;17:2401–8.
[29] McAdoo BG, Quak M, Gnyawali KR, Adhikari BR, Devkota S, Rajbhandari PL, et al. Roads and landslides in Nepal: how development affects environmental risk. Nat Hazards Earth Syst Sci. 2018;18:3203–10. https://doi.org/10.5194/nhess-18-3203-2018.
[30] Meena SR, Tavakkoli Piralilou S. Comparison of earthquake-triggered landslide inventories: a case study of the 2015 Gorkha earthquake, Nepal. Geosciences. 2019;9(10): 437–54.
[31] Meunier P, Hovius N, Haines JA. Topographic site effects and the location of earthquake induced landslides. Earth Planet Sci Lett. 2008;275(3–4):221–32.
[32] Milledge DG, Densmore AL, Bellugi D, Rosser NJ, Watt J, Li G, et al. Simple rules to minimise exposure to coseismic landslide hazard. Nat Hazards Earth Syst Sci. 2019;19: 837–56.
[33] Oven K, Rana S, Basyal GK, Rosser N, Kincey M. Policies, politics and practices of landslide risk management in post-earthquake Nepal: perspectives from above and below. In: Hutt M, Leichty M, Lotter S, editors. Epicentre to aftermath: rebuilding and remembering in the wake of Nepal's earthquakes. Delhi: Cambridge University Press; 2020.
[34] Owen LA, Kamp U, Khattak GA, Harp EL, Keefer DK, Bauer MA. Landslides triggered by the 8 October 2005 Kashmir earthquake. Geomorphology. 2008;94(1–2):1–9.
[35] Parker RN, Hancox GT, Petley DN, Massey CI, Densmore AL, Rosser NJ. Spatial distributions of earthquake-induced landslides and hillslope preconditioning in northwest South Island, New Zealand. Earth Surf Dyn. 2015;3(4):501–25.
[36] Petley DN, Dunning SA, Rosser NJ, Kausar AB. Incipient landslides in the Jhelum Valley, Pakistan following the 8th October 2005 earthquake. In: Marui H, editor. Disaster mitigation of debris flows, slope failures and landslides. Frontiers in Science Series. Tokyo, Japan. Universal Academy Press; 2006. p. 47–56.
[37] Petley DN, Hearn GJ, Hart A, Rosser NJ, Dunning SA, Oven K, et al. Trends in landslide occurrence in Nepal. Nat Hazards. 2007;43:23–44.
[38] Qiu S, Zhu Z, He B. Fmask 4.0: improved cloud and cloud shadow detection in Landsats 4–8 and Sentinel-2 imagery. Remote Sens Environ. 2019;231:111–205.
[39] Rault C, Chao WA, Gelis C, Burtin A, Chang J-M, Marc O, et al. Seismic response of a mountain ridge prone to landsliding. Bull Seismol Soc Am. 2019. https://doi.org/10.1785/0120190127.
[40] Roback K, Clark MK, West AJ, Zekkos D, Li G, Gallen SF, et al. The size, distribution, and mobility of landslides caused by the 2015 Mw7. 8 Gorkha earthquake, Nepal. Geomorphology. 2018;301:121–38.
[41] Robinson TR, Rosser NJ, Densmore AL, Williams JG, Kincey ME, Benjamin J, et al. Rapid post-earthquake modelling of coseismic landslide magnitude and distribution for emergency response decision support. Nat Hazards Earth Syst Sci. 2017;17:1521–40.
[42] Stähli M, Sättele M, Huggel C, McArdell BW, Lehmann P, Van Herwijnen A, et al. Monitoring and prediction in early warning systems for rapid mass movements. Nat Hazards Earth Syst Sci. 2015;15:905–17.
[43] Sudmeier-Rieux K, McAdoo BG, Devkota S, Rajbhandari PCL, Howell J, Sharma S. Invited perspectives: mountain roads in Nepal at a new crossroads. Nat Hazards Earth Syst Sci. 2019;19:655–60.
[45] Tanyaş H, van Westen CJ, Allstadt KE, Anna Nowicki Jessee M, Görüm T, Jibson RW, et al. Presentation and analysis of a worldwide database of earthquake-induced landslide inventories. J Geophys Res Earth. 2017;122:1991–2015.
[46] Tiwari B, Ajmera B, Dhital S. Characteristics of moderate-to large-scale landslides triggered by the Mw 7.8 2015 Gorkha earthquake and its aftershocks. Landslides. 2017; 14(4):1297–318.
[47] Wang J, Jin Z, Hilton RG, Zhang F, Densmore AL, Li G, et al. Controls on fluvial evacuation of sediment from earthquake-triggered landslides. Geology. 2015;43:115–8.
[48] Weiss DJ, Walsh SJ. Remote sensing of mountain environments. Geogr Compass. 2009;3 (1):1–21.
[49] Williams JG, Rosser NJ, Kincey ME, Benjamin J, Oven KJ, Densmore AL, et al. Satellite-based emergency mapping using optical imagery: experience and reflections from the 2015 Nepal earthquakes. Nat Hazards Earth Syst Sci. 2018;18:185–205.
[50] World Bank. Nepal environment sector diagnostic: Path to sustainable growth under federalism. Country Environmental Analysis. Washington, DC: World Bank; 2019.
[51] Xu C, Xu X, Tian Y, Shen L, Yao Q, Huang X, et al. Two comparable earthquakes produced greatly different coseismic landslides: the 2015 Gorkha, Nepal and 2008 Wenchuan, China events. J Earth Sci. 2016;27(6):1008–15.
[52] Yunus AP, Fan X, Tang X, Jie D, Xu Q, Huang R. Decadal vegetation succession from MODIS reveals the spatio-temporal evolution of post-seismic landsliding after the 2008 Wenchuan earthquake. Remote Sens Environ. 2020;236:111476.
[67] Zhou W, Tang C. Rainfall thresholds for debris flow initiation in the Wenchuan earthquake-stricken area, southwestern China. Landslides. 2014;11:877–87 https://doi.org/10.1007/s10346-013-0421-5.